BJD
British Journal of Dermatology

Fibroblast activation and abnormal extracellular matrix remodelling as common hallmarks in three cancer-prone genodermatoses*

E. Chacón-Solano,[1,2] C. León,[1,2] F. Díaz,[1,2] F. García-García,[3] M. García,[1,2,4] M.J. Escámez,[1,2,4] S. Guerrero-Aspizua,[1,2,4] C.J. Conti,[1,2] Á. Mencía,[1,2] L. Martínez-Santamaría,[1,2] S. Llames,[2,4,5] M. Pévida,[5] J. Carbonell-Caballero,[6] J.A. Puig-Butillé,[7] R. Maseda,[8] S. Puig,[7] R. de Lucas,[8] E. Baselga,[9] F. Larcher,[1,2,4] J. Dopazo[10,11,12] and M. del Río[1,2,4]

[1]Department of Bioengineering, Universidad Carlos III de Madrid, Madrid, Spain
[2]Regenerative Medicine and Tissue Engineering Group, Fundación Jiménez Díaz (IIS-FJD), Madrid, Spain
[3]Bioinformatics and Biostatistics Unit and [6]Department of Computational Genomics, Centro de Investigación Príncipe Felipe (CIPF), Valencia, Spain
[4]Epithelial Biomedicine Division, CIEMAT-CIBERER (U714), Madrid, Spain
[5]Tissue Engineering Unit, Centro Comunitario Sangre y Tejidos (CCST), Oviedo, Spain
[7]Melanoma Unit, Hospital Clinic & IDIBAPS (Institut d'Investigacions Biomèdiques Agustí Pi i Sunyer), CIBERER (U726), Universitat de Barcelona, Barcelona, Spain
[8]Department of Pediatric Dermatology, La Paz Hospital, Madrid, Spain
[9]Department of Pediatric Dermatology, Santa Creu I Sant Pau Hospital, Barcelona, Spain
[10]Clinical Bioinformatics Area, Fundación Progreso y Salud, CDCA, Hospital Virgen del Rocío, Sevilla, Spain
[11]Functional Genomics Node, INB-ELIXIR-es, FPS, Hospital Virgen del Rocío, Sevilla, Spain
[12]Bioinformatics in Rare Diseases (BiER-U715), CIBERER, FPS, Hospital Virgen del Rocío, Sevilla, Spain

Linked Comment: Has. Br J Dermatol 2019; **181**:440–441.

Summary

Background Recessive dystrophic epidermolysis bullosa (RDEB), Kindler syndrome (KS) and xeroderma pigmentosum complementation group C (XPC) are three cancer-prone genodermatoses whose causal genetic mutations cannot fully explain, on their own, the array of associated phenotypic manifestations. Recent evidence highlights the role of the stromal microenvironment in the pathology of these disorders.

Objectives To investigate, by means of comparative gene expression analysis, the role played by dermal fibroblasts in the pathogenesis of RDEB, KS and XPC.

Methods We conducted RNA-Seq analysis, which included a thorough examination of the differentially expressed genes, a functional enrichment analysis and a description of affected signalling circuits. Transcriptomic data were validated at the protein level in cell cultures, serum samples and skin biopsies.

Results Interdisease comparisons against control fibroblasts revealed a unifying signature of 186 differentially expressed genes and four signalling pathways in the three genodermatoses. Remarkably, some of the uncovered expression changes suggest a synthetic fibroblast phenotype characterized by the aberrant expression of extracellular matrix (ECM) proteins. Western blot and immunofluorescence *in situ* analyses validated the RNA-Seq data. In addition, enzyme-linked immunosorbent assay revealed increased circulating levels of periostin in patients with RDEB.

Conclusions Our results suggest that the different causal genetic defects converge into common changes in gene expression, possibly due to injury-sensitive events. These, in turn, trigger a cascade of reactions involving abnormal ECM deposition and underexpression of antioxidant enzymes. The elucidated expression signature provides new potential biomarkers and common therapeutic targets in RDEB, XPC and KS.

Correspondence
Fernando Larcher; Joaquin Dopazo; Marcela Del Río.
E-mails: fernando.larcher@ciemat.es; joaquin.dopazo@juntadeandalucia.es; mrnechae@ing.uc3m.es

Accepted for publication
24 January 2019

Funding sources
This study was supported by grants from the Spanish Ministry of Economy and Competitiveness (SAF2013-43475R, SAF2017-88908-R and SAF2017-86810-R); from Instituto de Salud Carlos III and CIBERER, cofunded with European Regional Development Funds (ERDF) (PT13/0001/0007, PI14/00931, PI15/00716, PI15/00956, PT17/0009/0006 and PI17/01747); and from the European Union (HEALTH-F2-2011-261392 and H2020-INFRADEV-1-2015-1/ELIXIR-EXCELERATE-ref.676559). Additional funding from Comunidad de Madrid (AvanCell-CM S2017/BMD-3692); Catalan Government (AGAUR 2014_SGR_603); 'Fundació La Marató de TV3, 201331-30'; CERCA Programme/Generalitat de Catalunya; and 'Fundación Científica de la Asociación Española Contra el Cáncer', Spain.

Conflicts of interest
None to declare.

E.C.S., C.L. and F.D. contributed equally

*Plain language summary available online

DOI 10.1111/bjd.17698

What's already known about this topic?

- Recessive dystrophic epidermolysis bullosa (RDEB), Kindler syndrome (KS) and xeroderma pigmentosum complementation group C (XPC) are three genodermatoses with high predisposition to cancer development.
- Although their causal genetic mutations mainly affect epithelia, the dermal microenvironment likely contributes to the physiopathology of these disorders.

What does this study add?

- We disclose a large overlapping transcription profile between XPC, KS and RDEB fibroblasts that points towards an activated phenotype with high matrix-synthetic capacity.
- This common signature seems to be independent of the primary causal deficiency, but reflects an underlying derangement of the extracellular matrix via transforming growth factor-β signalling activation and oxidative state imbalance.

What is the translational message?

- This study broadens the current knowledge about the pathology of these diseases and highlights new targets and biomarkers for effective therapeutic intervention.
- It is suggested that high levels of circulating periostin could represent a potential biomarker in RDEB.

The progress made in molecular genetics has greatly contributed to identifying the primary causes of a large number of heritable skin diseases.[1] However, these findings do not always explain by themselves the complex phenotypic manifestations observed in cancer-prone genodermatoses, such as recessive dystrophic epidermolysis bullosa (RDEB), Kindler syndrome (KS) and xeroderma pigmentosum complementation group C (XPC). RDEB is caused by loss-of-function mutations in the *COL7A1* gene, which encodes type VII collagen (C7) anchoring fibrils, structures that connect the epidermal basement membrane to the dermal tissue. C7 deficiency causes loss of dermoepidermal adhesion, resulting in blister formation, scarring and aggressive carcinoma development.[2]

KS results from recessive mutations in the *FERMT1* gene, encoding kindlin-1. This protein mediates anchorage between the actin cytoskeleton and the extracellular matrix (ECM) via focal adhesions. KS is characterized clinically by early-age acral skin blisters, photosensitivity and high risk of mucocutaneous malignancies.[3–5] XPC is characterized by mutations in the *XPC* gene, which cause a severe deficiency in the nucleotide excision repair pathway. Patients with XPC are highly sensitive to ultraviolet radiation and have a very high risk of developing skin tumours in sun-exposed areas, mostly basal and squamous cell carcinomas arising from epidermal keratinocytes, and malignant melanomas.[6] Patients with XPC also have a high risk of developing tumours in internal organs not exposed to sunlight.[7]

Besides cancer susceptibility, other common clinical signs to the three genodermatoses are inflammation and premature skin ageing.[8–10] Although the specific primary and subsequent genetic alterations at the epidermal level are likely to be major drivers for carcinogenesis in these disorders, an altered stroma may play a facilitating role towards tumour development and malignant progression.

Robust data, gathered mainly from omics studies of patient cells and mouse models, underscore the role of aberrant ECM deposition, leading to progressive fibrosis and cutaneous squamous cell carcinoma (cSCC) in RDEB. This process appears to be mediated by the dermal fibroblasts, which acquire molecular changes similar to those present in the tumour microenvironment (i.e. cancer-associated fibroblasts; CAFs).[11] Less is known in this regard for KS and XPC, although marginal evidence indicates that fibroblasts may also be relevant in the disease pathogenesis.[12–15] Here we demonstrate through RNA-Seq analysis and expression validation of relevant genes that RDEB, XPC and KS fibroblasts allow establishment of a common profibrotic microenvironment that could favour disease progression and cancer.

Materials and methods

Sample collection and cell culture

All procedures were approved by the ethics committee of La Paz University Hospital (code HULP: PI-1602) and were conducted

in accordance with the Declaration of Helsinki and subsequent revisions. Skin biopsies from unaffected areas of seven healthy donors, 11 patients with RDEB, four patients with KS and four patients with XPC were obtained after written informed consent was obtained. Fibroblasts were isolated by mechanical and enzymatic digestion as previously described.[16] They were cultured in Dulbecco's Modified Eagle's Medium supplemented with 10% fetal bovine serum (both Thermo Fisher Scientific, Waltham, MA, U.S.A. and Invitrogen, Carlsbad, CA, U.S.A.) and 1% Antibiotic-Antimycotic (Thermo Fisher Scientific). The characteristics of the patients and controls can be seen in Table S1 (see Supporting Information). All cells used were at early three to seven passages (see Table S1).

RNA extraction

Culture medium was changed 24 h before harvesting the cells. Total RNA was isolated from confluent primary fibroblasts using an RNeasy Kit (Qiagen, Hilden, Germany) according to the manufacturer's protocol recommendations. RNA concentration and quality were determined on a NanoDrop Spectrophotometer (Thermo Scientific Inc.) and integrity was verified with a Bioanalyzer 2100 (Agilent, Santa Clara, CA, U.S.A.). The RNA integrity number in all cases was higher than 8·5. To minimize technical variability, RNA extracts from four technical replicates of each sample were mixed.

RNA-Seq data processing

cDNA libraries were generated for each sample using the TruSeq RNA Sample Preparation Kit (Illumina, San Diego, CA, U.S.A.) according to the recommended protocol. Ligation and library integrity were verified using an Agilent Bioanalyzer 2100. Sample libraries ligated with unique adapter sequences were multiplexed six to a lane and were sequenced by Edinburgh Genomics (Edinburgh, U.K.) using Illumina HiSeq HO v4 125 paired end sequencing. Quality control analysis on the resulting FASTQ files was performed using FastQC (Babraham Bioinformatics, Cambridge, U.K.). Reads were adapter trimmed using cutadapt version 1·3 (https://pypi.org/project/cutadapt/1·3) with the parameters -q 30 -m 50 -a AGATCGGAAGAGC. Trimmed reads were aligned to Ensembl version 38·81 of the *Homo sapiens* genome with TopHat2 version 2·0·13 (https://ccb.jhu.edu/software/tophat) using default parameters, except '-r -70 -mate-std-dev 75' to specify insert sizes. The BAM files were sorted by name using Picard-tools version 1·115 SortSam (https://broadinstitute.github.io/picard). Read counts were generated using HTSeq-count version 0·6·0 in unstranded mode (https://htseq.readthedocs.io) and Python version 2·7·3, with parameters -m union -i gene_id -t exon. Raw and processed data are stored at the National Center for Biotechnology Information's Gene Expression Omnibus, accession code https://www.ncbi.nlm.nih.gov/geo/query/acc.cgi?acc=GSE119501.

RNA-Seq data were normalized using the Trimmed Mean of M-values.[17] An adjustment for possible batch effects was performed using the R package ComBat.[18] The transcripts that had an average expression per condition < 1 count per million and a coefficient of variation per condition > 100% were filtered. Differential expression analysis was performed with the Bioconductor package edgeR.[19] The conventional multiple-testing P-value correction procedure proposed by Benjamini and Hochberg was used to derive adjusted P-values.[20] Enrichment analysis was carried out for the gene ontology terms using the Babelomics suite[21] and DAVID bioinformatic resources.[22]

Pathway activity analysis and protein–protein interaction

The signalling circuit activity analysis method,[23] as implemented in the hiPathia R package (https://github.com/babelomics/hipathia), was applied to all disease vs. healthy control comparisons. Under this modelling schema, signalling circuits are defined within Kyoto Encyclopedia of Genes and Genomes (KEGG) pathways as the chain of proteins that connect a receptor protein to an effector protein that triggers specific cellular activities. The signal is propagated from the receptor protein along the proteins that compose the circuit by a recursive formula that takes into account the activity of both activator and inhibitor proteins. Finally, the list of the common dysregulated genes in all disease vs. control comparisons was uploaded to STRING,[24] a database that represents the known protein–protein interactions (PPIs). The minimum required interaction score was set to > 0·7, allowing only high-confidence connections between nodes.

Western blot analysis

Primary fibroblasts, serum starved for 24 h, were lysed with 25-mmol L^{-1} Tris-HCl (pH 7·4), 100-mmol L^{-1} NaCl, 1% Nonidet P-40 and protease inhibitor cocktail (Roche Diagnostics Limited, Burgess Hill, U.K.). The extracts were cleared of cellular debris by centrifugation at 16 000 ***g*** for 15 min at 4 °C. Protein extracts were electrophoresed on sodium dodecylsulfate polyacrylamide 4–12% Bis-Tris gel and transferred onto nitrocellulose membranes. The membranes were blocked with 5% nonfat milk powder in 1X Tris-buffered saline for 1 h at room temperature and incubated overnight with one of the following antibodies: antitenascin C (MAB2138; R&D Systems Inc., Minneapolis, MN, U.S.A.), anti-βIG-H3 (D31B8; Cell Signaling Technology, Beverly, MA, U.S.A.), anti-ALDH1A1 (EP1933Y; Abcam, Cambridge, U.K.), antiperiostin (sc-398631) antifibulin-1 (sc-25281), anti-TGase2 (sc-48387) and anti-GAPDH (sc-25778; all Santa Cruz Biotechnology, Santa Cruz, CA, U.S.A.). Detection was performed using horseradish peroxidase-conjugated secondary antibodies and a chemiluminescent detection assay (SuperSignal West, Thermo Fisher Scientific). Three independent experiments were performed for each patient sample and control.

Immunofluorescence analysis

Skin cryosections from three healthy donors, two patients with RDEB and two patients with KS were immunostained against

tenascin C (MAB2138) and periostin (sc-398631). Fluorescence quantification was measured using the ImageJ program (https://imagej.nih.gov/ij). Student's t-test was applied to compare the fluorescence intensity/area means of samples, using GraphPad Prism 5·04 (GraphPad Software, La Jolla, CA, U.S.A.).

Enzyme-linked immunosorbent assay

Serum samples from 16 patients with RDEB and 10 healthy donors (Table S1b; see Supporting Information) were analysed using a human periostin enzyme-linked immunosorbent assay kit (EHPOSTN-PL; Thermo Fisher Scientific) according to the manufacturer's protocol. The absorbance was measured at 450 nm and 550 nm with a microtitre plate reader (Tecan Genios Pro; Tecan Austria GmbH, Grödig, Austria). The D'Agostino–Pearson omnibus test was applied to determine whether the values had a normal distribution. An unpaired t-test with Welch's correction was done to determine the statistical significance between patients with RDEB and controls (in GraphPad Prism 5·04). Two independent experiments were performed for each patient sample and for controls.

Results

Patients with genodermatoses and mutations

Patients were screened for *COL7A1*, *XPC* and *FERMT1* specific mutations, according to the diagnosed disease (Table S1a; see Supporting Information). All patients with RDEB were homozygous for a *COL7A1* recurrent mutation (c.6527insC), leading to a premature termination codon.[25] All of the screened patients with XPC carried a homozygous frameshift mutation (c.1643_1644delTG) in *XPC*, resulting in a premature termination codon. Finally, patients with KS were the most heterogeneous group, with three different homozygous mutations in *FERMT1*. Sample KS1 produced altered splicing due to insertion of a new triplet (c.1371+4>G), KS2 has a missense variant (c.1198T>C) and KS3 has a frameshift mutation (c.676dupC).

Identification of common expression signatures linked to fibroblast activation and extracellular matrix deposition

RNA-Seq counts were obtained for primary fibroblasts isolated from three healthy donors, nine patients with RDEB, three patients with KS and three patients with XPC. In total 22 970 transcripts, identified by their Ensembl IDs, were obtained for each sample after data quality assessment and normalization (Table S2; see Supporting Information). The observed arrangement of the samples in the principal component analysis discarded any possible batch effect and organized the samples following the different disease groups. Notably, all genodermatosis samples are located in proximity within the plot, and are distinctly separated from controls (Fig. 1a), pointing towards a similar transcription profile between the three genodermatoses.

In order to identify the dysregulated genes, differential expression analysis was carried out, contrasting each disease group (RDEB, KS or XPC) vs. healthy controls (Table S3). The number of differentially expressed genes (false discovery rate $< 0{\cdot}05$) in the different comparisons is detailed in Table 1. A Venn diagram of the different comparisons revealed an intersection of 227 common dysregulated transcripts (containing 186 genes) in the three genodermatoses (Fig. 1b). Interestingly, all of these transcripts (129 upregulated and 98 downregulated) showed not only the same expression pattern (Fig. 1c), but also an impressive positive correlation between the fold changes (Fig. 1d). This suggests that the common expression profile may have a similar phenotypic impact on the three diseases.

Common expression patterns are best understood through the examination of enriched gene ontology terms[26] and KEGG pathways.[27] This approach provides an undirected method to highlight those biological mechanisms that could be potentially relevant to the diseases. The output of this enrichment analysis is a list of pathways and/or ontologies that involve a statistically significant number of dysregulated genes, associated with the same biological mechanism (Fig. 2, Table S4; see Supporting Information).

Enriched gene ontology terms for all of the diseases point towards an abnormal relationship between the cell and its stroma. This suggests that the contribution of dermal fibroblasts to the disease lies in the altered response they exert on the surrounding microenvironment. The dysregulated genes were significantly associated with ECM and the cell periphery (cellular component). Furthermore, glycosaminoglycan binding, sulfur compound binding and heparin binding – which point towards ECM components – are over-represented (molecular function). Apart from these terms, altered activity of transcription factors is also noticeable, presumably associated with the observed differences in gene transcription. KEGG pathway analysis identified common alterations in phosphoinositol-3-kinase (PI3K)–Akt signalling, the chemokine repertoire and two cancer-related pathways (highlighted terms in Table S4; see Supporting Information).

To gain a deeper insight into the altered mechanisms, we employed the web tool hiPathia (http://hipathia.babelomics.org) to decompose KEGG pathways into signalling circuits, by transforming gene expression profiles into signal transduction activity profiles.[23] We found 42 overlapping circuits in the three genodermatoses when comparing them against controls (Fig. S1a; see Supporting Information). Effectors were associated with cell proliferation (*AREG*, *MAPK8*), transforming growth factor (TGF)-β signalling (*PITX2*) and ECM–cell interactions (*PLAU*, *MAP3K4*) (highlighted terms in Table S5; see Supporting Information). A particular example of these circuits includes activation of *BCL2* – an effector molecule with an antiapoptotic effect – initiated in multiple overexpressed nodes and propagated through the PI3K–Akt pathway (Fig. S1b; see Supporting Information).

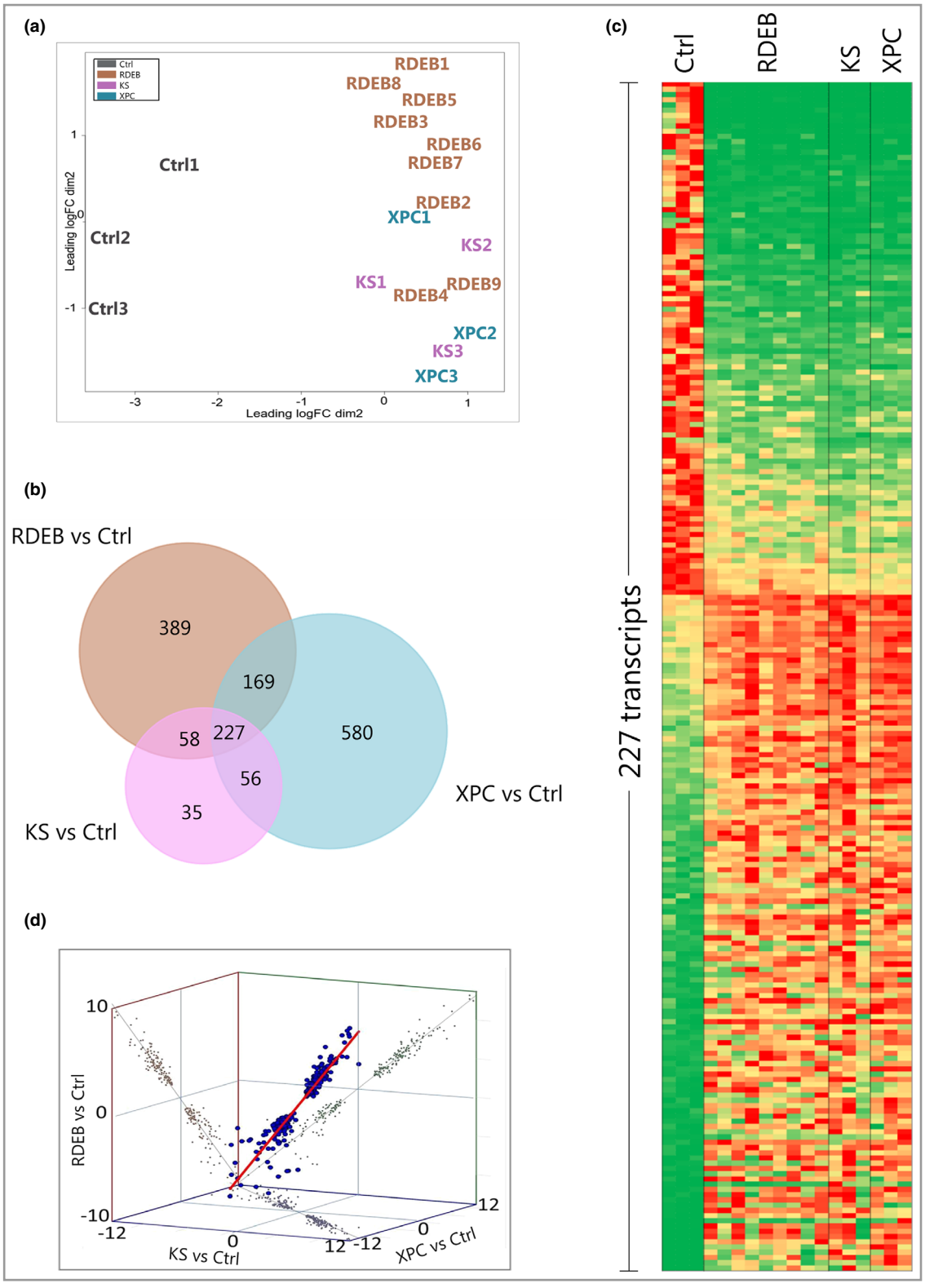

Fig 1. Differential gene expression profile. (a) Principal component analysis plot representing the global distribution of each sequenced sample, after data processing and normalization. Disease samples tended to group together and distantly from the controls. (b) An overlapping set of 227 transcripts commonly dysregulated in all of the diseases. (c) Heat map of the normalized expression of the 227 transcripts (red, upregulated; green, downregulated in the disease). (d) Linear regression of fold changes of the 227 transcripts (blue dots) shows an impressive positive correlation (R^2 = 0·895). Axes indicate the fold-change values (logarithmic scale). RDEB, recessive dystrophic epidermolysis bullosa; KS, Kindler syndrome; XPC, xeroderma pigmentosum complementation group C; Ctrl, healthy control.

Table 1 Number of genes differentially expressed in each genodermatosis vs. healthy controls

Comparison	Underexpressed	Overexpressed	Total
RDEB vs. control	516	327	843
KS vs. control	196	180	376
XPC vs. control	523	509	1032

RDEB, recessive dystrophic epidermolysis bullosa; KS, Kindler syndrome; XPC, xeroderma pigmentosum complementation group C.

To identify functional associations between the 186 differentially expressed genes, the STRING database[24] was used to generate PPI networks. The enrichment PPI P-value (0·0013) indicates that the commonly altered genes do not represent a randomly scattered set of proteins, but a meaningfully connected set of genes in accordance with their biological functions. Three major clusters (A, B and C) of proteins were detected (Fig. 3). Cluster A includes a group of proteins, mostly downregulated, involved in signalling pathways and signal transduction (e.g. *JAK3*, *PTK2B* and *PRKCQ*). Interestingly, this cluster also contains the angiotensin II receptor (*AGTR1*, upregulated), a target of recent antifibrotic therapy tested in RDEB,[28] and the antioxidant enzyme extracellular superoxide dismutase (*SOD3*, downregulated), previously proposed as a repressor molecule of skin inflammation.[29]

Cluster B is formed predominantly by a group of transcription factors (e.g. *PITX2*, a procollagen lysyl hydroxylase transcription factor). Cluster C is represented by matrisome and matrisome-associated genes (http://matrisomeproject.mit.edu),[30] implicated in the stabilization, deposition and remodelling of the ECM (e.g. *TGFBI*, *FN1*, *TNC* and *POSTN*). Among the minor-clustered nodes, downregulation of the *ALDH1A1* gene received our attention. This gene encodes an antioxidant enzyme (aldehyde dehydrogenase 1A1) related

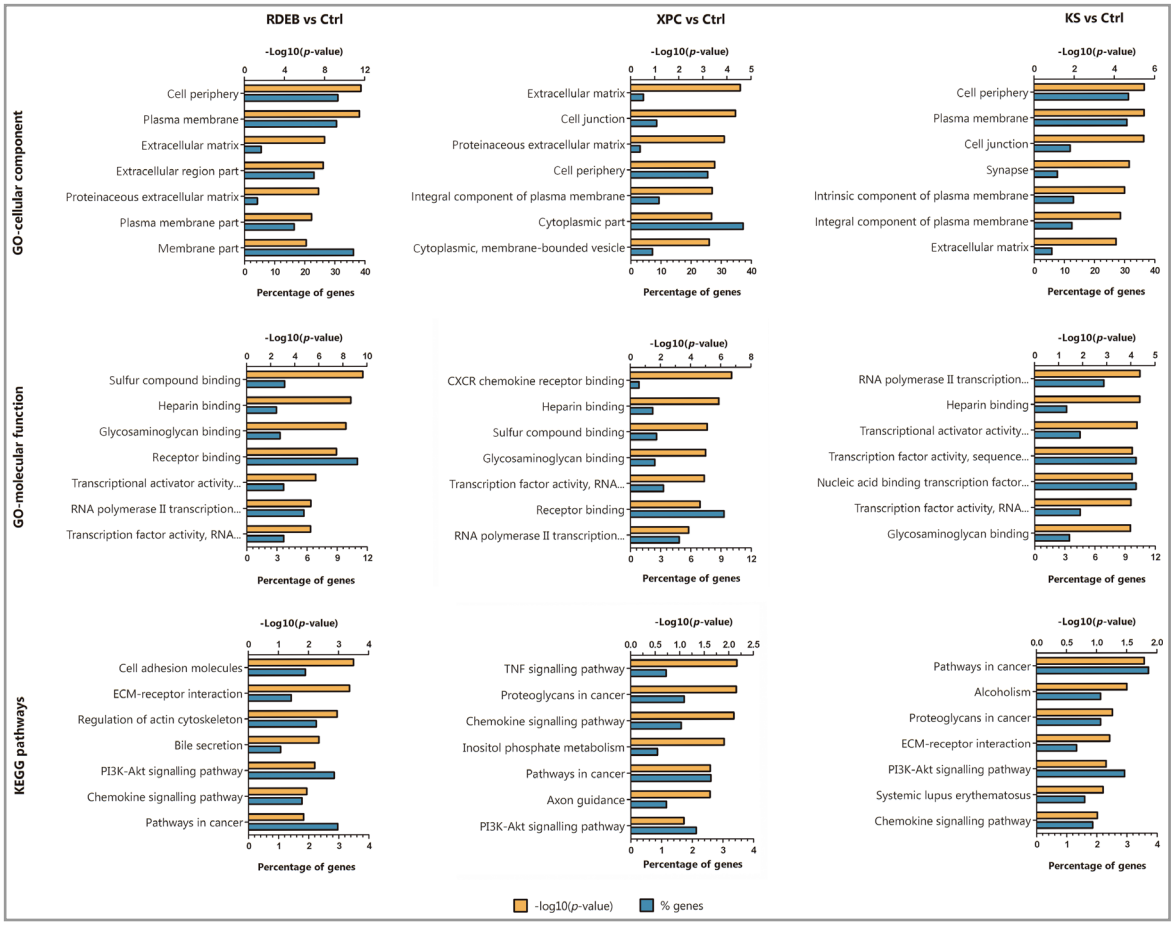

Fig 2. Enrichment analysis of differentially expressed genes. Within the specific alterations of each disease, enriched gene ontology (GO) terms highlight common abnormalities in the three genodermatoses with respect to cell periphery, extracellular matrix (ECM) and activity of transcription factors. Kyoto Encyclopedia of Genes and Genomes (KEGG) pathways reveal enriched categories related with cancer, phosphoinositol-3-kinase (PI3K)–Akt and chemokine signalling. The highest-ranked categories in each disease are shown according to the P-value and percentage of genes. RDEB, recessive dystrophic epidermolysis bullosa; KS, Kindler syndrome; XPC, xeroderma pigmentosum complementation group C; Ctrl, healthy control; TNF, tumour necrosis factor.

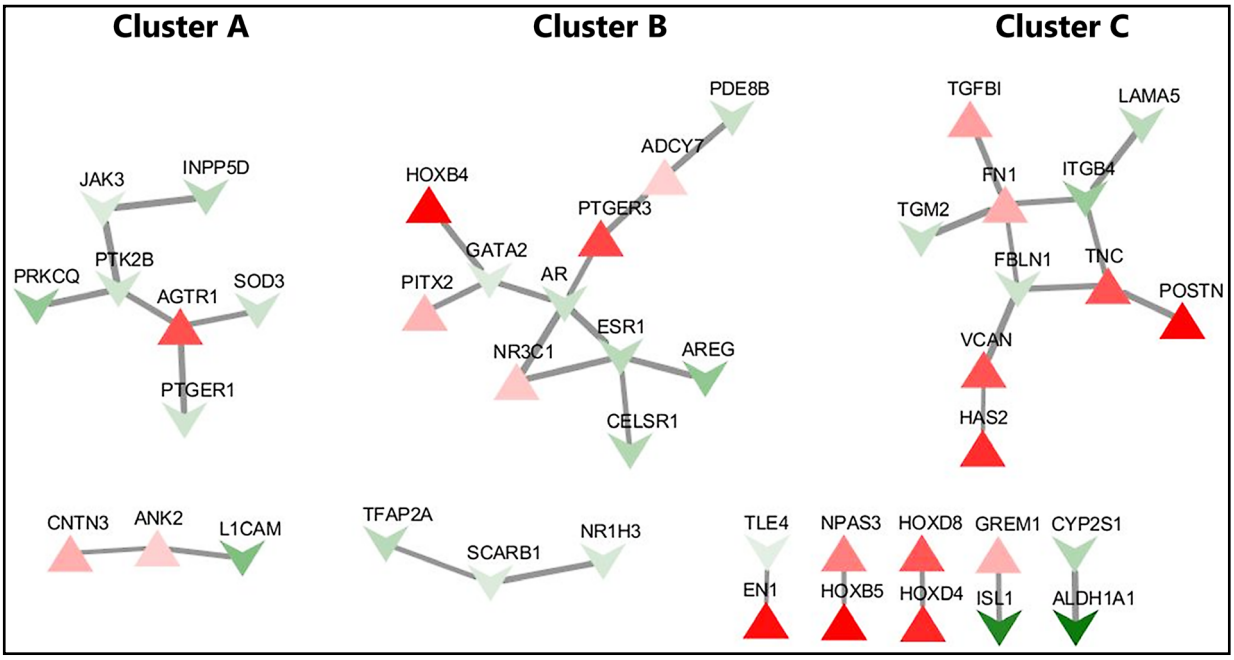

Fig 3. Protein–protein interaction network of the common dysregulated genes. The three largest connected components, labelled as clusters A, B and C, represent clusters of highly connected, biologically related proteins. The node colour is graded according to the average fold change (red, upregulated; green, downregulated in the disease). The edge width is proportional to the STRING interaction score, which represents the confidence for that interaction. Groups of potentially interactive proteins with fewer nodes are shown below the main clusters. Proteins without interactions are not shown. The average node degree is 0·387 and the average local clustering coefficient is 0·158.

to ultraviolet protection against oxidative stress[31] and is repressed by TGF-β.[32] In our analysis, *ALDH1A1* is one of the most significantly underexpressed genes in the three diseases.

Validation of altered gene expression

Given the importance of the extracellular component – evidenced by enriched gene ontology terms and KEGG pathways – we took advantage of the STRING PPI and chose several proteins of cluster C for validation by Western blot (Fig. 4). In this analysis we included additional patient and control samples not used for RNA-Seq (Table S1b; see Supporting Information). In accordance with the transcriptomic data, fibulin-1, transglutaminase-2 and ALDH1A1 were underexpressed in the diseases, while expression of tenascin C, periostin and TGF-β induced (TGF-βI) was increased. In addition to the changes observed in these markers, we found high levels of α-smooth muscle actin in all fibroblasts of all genodermatoses, confirming their activated phenotype (data not shown). Variability in protein expression levels in individual fibroblasts was observed; however, there was no evident pattern associated with body sites of origin or the age of the donors. Abnormal expression of some of these proteins has previously been described in RDEB fibroblasts,[33] but not the periostin overexpression. Thus, we decided to study their expression by immunofluorescence in available skin biopsy sections from patients with RDEB and KS. The analysis showed a degree and pattern of overexpression similar to those seen in tenascin C, used as a positive control (Fig. 5).

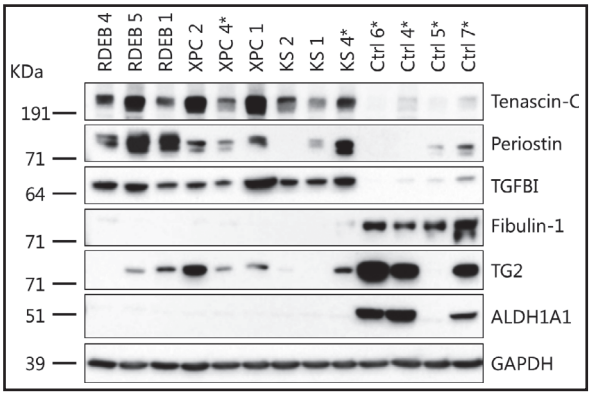

Fig 4. Western blot validation of relevant genes. Immunoblot analysis of fibroblast cell lysates confirms the high expression of tenascin C, periostin and transforming growth factor-β induced (TGFBI), together with underexpression of transglutaminase-2 (TG2), aldehyde dehydrogenase 1A1 (ALDH1A1) and fibulin-1 in samples from patients with recessive dystrophic epidermolysis bullosa (RDEB), xeroderma pigmentosum complementation group C (XPC) and Kindler syndrome (KS). Glyceraldehyde-3-phosphate dehydrogenase (GAPDH) was used as the loading control. Samples not included in the RNA-Seq analysis are indicated by an asterisk (*). Ctrl, healthy control.

Identification of serum periostin as a novel biomarker in recessive dystrophic epidermolysis bullosa

Increased levels of circulating periostin have been shown in several noninherited fibrotic conditions including cancer.[34,35] Considering the overexpression of periostin seen *in vitro* and *in situ*, we subsequently searched for periostin in available serum samples of patients with RDEB and healthy donors. Consistently with the validation results, the mean ± SEM circulating periostin concentration was remarkably higher in patients with RDEB (65·7 ± 14·8 ng mL^{-1}; n = 16) than in controls (3·72 ± 0·33 ng mL^{-1}; n = 10) ($P < 0·001$; Fig. 6). This result suggests that periostin may represent a potential biomarker in RDEB.

Discussion

Here we conducted a global gene expression analysis of dermal fibroblasts – isolated from uninvolved skin areas of patients with XPC, KS and RDEB – with the goal of elucidating overlapping pathomechanisms in these cancer-prone genodermatoses. Despite each disease's gene expression singularities, our study allowed us to identify a common signature of 227 transcripts and four KEGG pathways differentially expressed against healthy controls. Our different bioinformatic analyses revealed the presence of three major determinants of an activated fibroblast phenotype, namely increased cell survival, altered TGF-β signalling and abnormal ECM remodelling.[36,37] It is known that fibroblasts become activated when they detect adverse cues from their surroundings (e.g. inflammation, mechanical trauma, TGF-β, oxidative stress) and acquire a proliferative phenotype characterized by aberrant secretion of ECM molecules.[38] Normally, activated fibroblasts return to their original state when the injury is resolved, through reprogramming or apoptosis.[39] However, if the insult becomes chronic, fibroblasts become irreversibly active, just as occurs in CAFs and fibrosis-associated fibroblasts.[40]

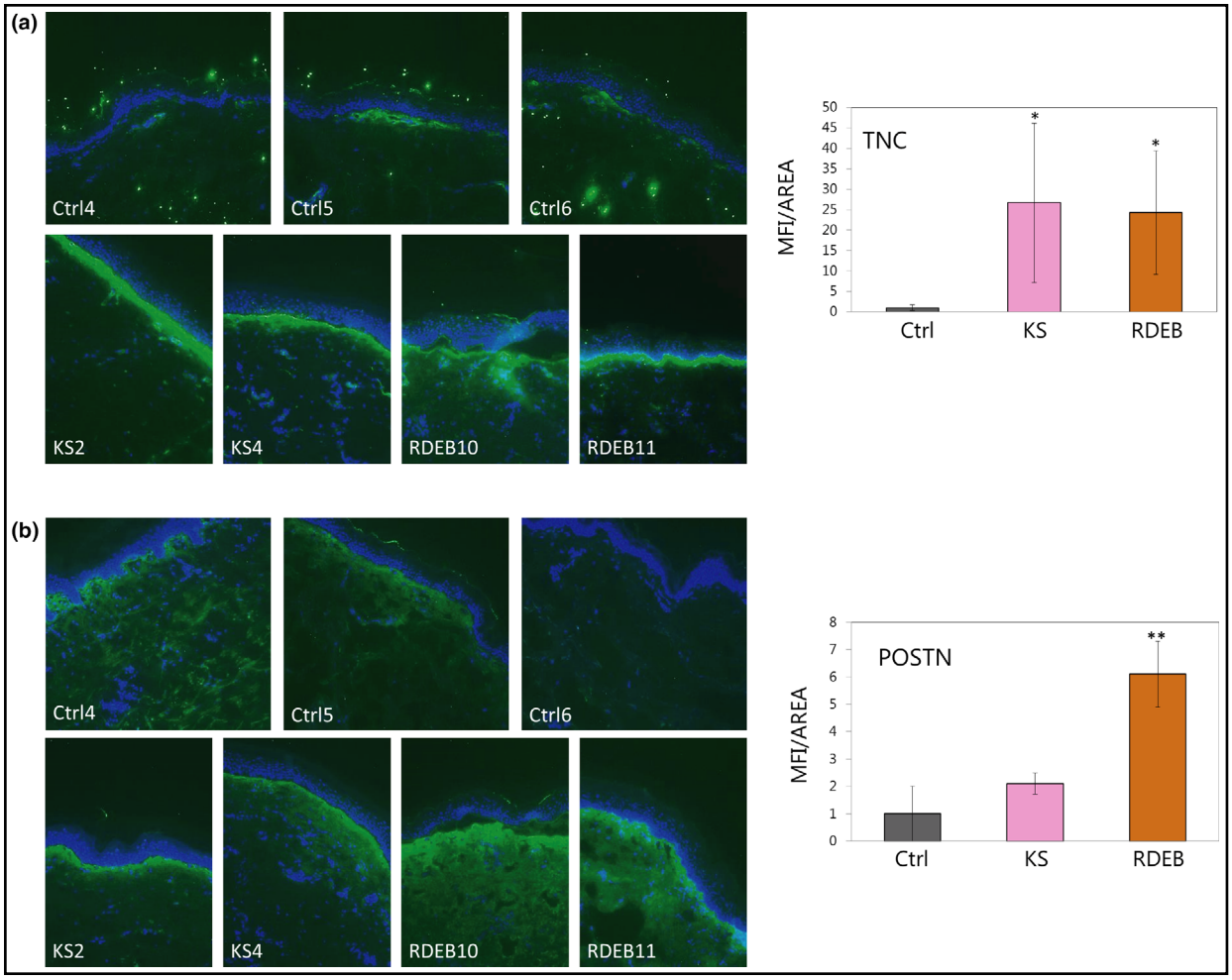

Fig 5. Immunofluorescence *in situ* validation of tenascin C (TNC) and periostin (POSTN). Skin biopsies sections from patients with recessive dystrophic epidermolysis bullosa (RDEB) and Kindler syndrome (KS) and healthy controls (Ctrl) were stained for (a) tenascin C and (b) periostin. Quantitation of fluorescence intensity was measured on five nonoverlapping microscopic fields per sample (ImageJ) and are represented as the mean ± SD staining intensity (MFI) per area value. The data were analysed by Student's t-test. *$P < 0·05$; **$P < 0·01$ vs. control.

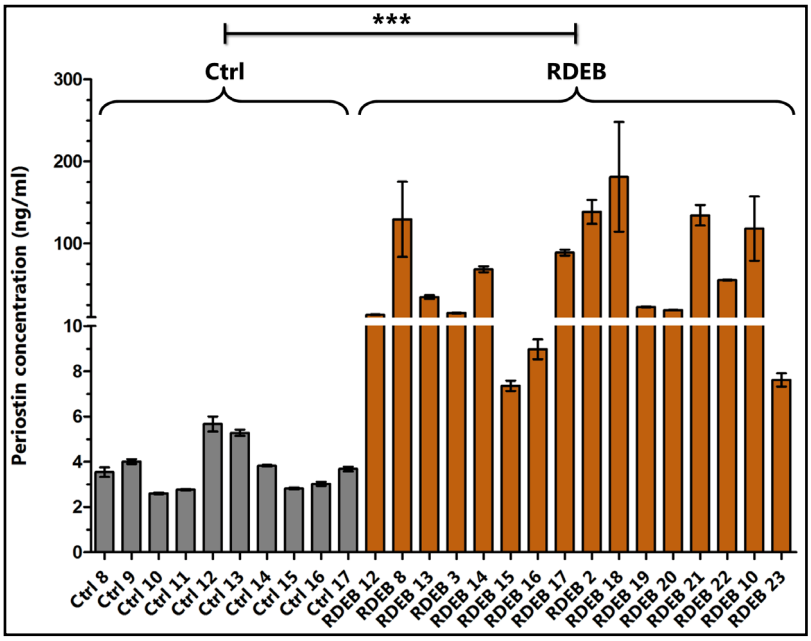

Fig 6. Circulating periostin levels in patients with recessive dystrophic epidermolysis bullosa (RDEB). The serum periostin concentration was significantly higher in patients with recessive dystrophic epidermolysis bullosa (mean ± SEM 65·7 ± 14·8 ng mL^{-1}; n = 16) than in donor controls (3·72 ± 0·33 ng mL^{-1}; n = 10). Two independent experiments were performed for each patient and control (Ctrl) sample. ***$P < 0·001$.

The pathway inference analysis highlighted several nodes involving PI3K–Akt signalling activation, ultimately triggering antiapoptotic and hyperproliferative stimuli via the BCL2 effector protein. Earlier studies on RDEB have also shown that increased PI3K–Akt signalling mediates cell survival and cSCC development. Indeed, it was proposed as one pharmacological target to prevent disease progression.[41] On the other hand, ontologies and categories referred to an altered activity of the cellular exterior, resulting in altered production of the chemokine repertoire and abnormal expression of the matrisome and matrisome-associated genes.

The involvement of aberrantly expressed ECM proteins (e.g. tenascin C, fibulin-1, transglutaminase-2 and TGF-βI) was previously associated with loss of C7.[33,42] Overexpression of tenascin C and TGF-β activation have also been shown in KS fibroblasts.[14] To our knowledge, abnormal expression of periostin has not yet been reported in nontumoral XPC, KS or RDEB fibroblasts, but it was recently shown in RDEB cSCC biopsies.[43] Periostin and tenascin C are induced by skin damage, promoting the activation of fibroblasts to repair the wound. Their overexpression has been linked to pathogenic roles in chronic inflammation, fibrosis and cancer.[34,44,45]

Different studies have shown that elevated levels of serum periostin are associated with progression and disease severity in pulmonary fibrosis,[46] colorectal cancer[47,48] and systemic sclerosis.[49] Our workflow from RNA-Seq to validation at the protein level allowed us to disclose periostin as a possible systemic biomarker, at least in RDEB (due to sample availability). Currently, several experimental antifibrotic therapies are under investigation for this disease.[28] Considering the paucity of available minimally invasive biomarkers to assess treatment efficacy, circulating periostin may be a useful molecule to consider. Further studies will be necessary to extend these results to XPC and KS.

A general inferred notion from previous studies was that causal defects, such as loss of C7 or kindlin-1, could be responsible for the abnormal ECM expression in RDEB and KS dermal fibroblasts.[14,50,51] However, without excluding a triggering effect due to the primary deficiencies, our results challenge the view of a direct genetic cause-driven effect. Rather, they stand for the existence of a shared injury-responsive event able to transduce the primary defect into epigenetic changes, leading to an activated phenotype (Fig. 7). A likely candidate appears to be TGF-β, as a large proportion of the common dysregulated genes (e.g. *TNC*, *POSTN*, *FN1*, *TGFBI* and *ALDH1A1*) are modulated by this factor. Another possible candidate, already shown in XPC and KS,[10,52–54] is oxidative stress, which could be able, by itself or through interaction with TGF-β, to trigger fibroblast activation and ECM accumulation.[55,56] In this context, downregulation of the *ALDH1A1* and *SOD3* genes, encoding antioxidant enzymes, could facilitate oxidative stress-induced damage. Similar expression changes in *ALDH1A1* were recently described as part of the myofibroblast-specific expression profile in mouse skin wounds.[57] In fact, an *in silico* comparison of our 186 dysregulated genes disclosed 41 overlapping genes included in the transcriptomic signature of mouse wound myofibroblasts. Overexpression of *POSTN* and *TNC* stands out among these 41 genes (Fig. S2; see Supporting Information).

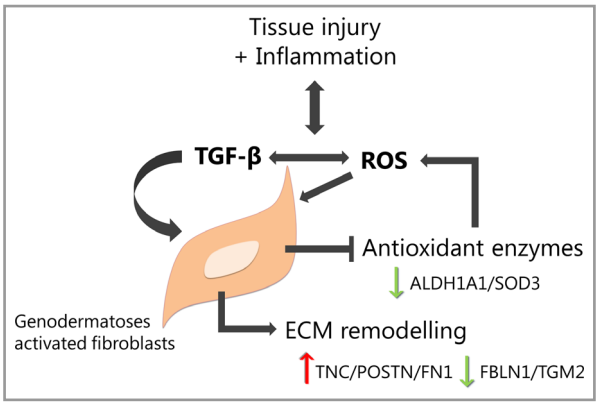

Fig 7. Model of the common pathomechanism suggested for recessive dystrophic epidermolysis bullosa (RDEB), xeroderma pigmentosum complementation group C (XPC) and Kindler syndrome (KS). Fibroblasts in the different genodermatoses respond similarly to tissue injury and inflammation. These persistent stimuli may converge into the activation of transforming growth factor (TGF)-β signalling and oxidative imbalance, which lead to overexpression of extracellular matrix (ECM) proteins (e.g. tenascin C, TNC; periostin, POSTN; and fibronectin 1, FN1) and reduced expression of antioxidant enzymes (e.g. aldehyde dehydrogenase 1A1, ALDH1A1; and superoxide dismutase, SOD3). Reciprocal regulation between TGF-β and reactive oxygen species (ROS) allows the acquisition of an activated and synthetic fibroblast phenotype and may promote disease progression. FBLN1, fibulin 1; TGM2, transglutaminase 2.

Examination of the exclusive transcriptional features of each disease may also offer interesting results, concerning the differential characteristics of each condition. However, these specific expression changes were not the focus of this study and should be considered separately. All in all, the common genetic signature in fibroblasts of the three genodermatoses shares some similarities with that found in myofibroblasts,[57] wound-activated fibroblasts and cutaneous CAFs.[11] The common mechanisms of the three diseases would allow consideration of symptom-relief therapies currently tested in RDEB to be used also in XPC and KS. In addition, newly elucidated molecular targets, such as those involved in derangement of the oxidative state, could be subject to novel pharmacological approaches.

References

1 DeStefano GM, Christiano AM. The genetics of human skin disease. *Cold Spring Harb Perspect Med* 2014; **4**:a015172.
2 Fine J-D, Bruckner-Tuderman L, Eady RAJ *et al.* Inherited epidermolysis bullosa: updated recommendations on diagnosis and classification. *J Am Acad Dermatol* 2014; **70**:1103–26.
3 Lotem M, Raben M, Zeltser R *et al.* Kindler syndrome complicated by squamous cell carcinoma of the hard palate: successful treatment with high-dose radiation therapy and granulocyte–macrophage colony-stimulating factor. *Br J Dermatol* 2001; **144**:1284–6.
4 Jobard F, Bouadjar B, Caux F *et al.* Identification of mutations in a new gene encoding a FERM family protein with a pleckstrin homology domain in Kindler syndrome. *Hum Mol Genet* 2003; **12**:925–35.
5 Siegel DH, Ashton GHS, Penagos HG *et al.* Loss of kindlin-1, a human homolog of the *Caenorhabditis elegans* actin–extracellular-matrix linker protein UNC-112, causes Kindler syndrome. *Am J Hum Genet* 2003; **73**:174–87.
6 Kraemer KH, Lee MM, Scotto J. Xeroderma pigmentosum. Cutaneous, ocular, and neurologic abnormalities in 830 published cases. *Arch Dermatol* 1987; **123**:241–50.
7 DiGiovanna JJ, Kraemer KH. Shining a light on xeroderma pigmentosum. *J Invest Dermatol* 2012; **132**:785–96.
8 Rezvani HR, Kim AL, Rossignol R *et al.* XPC silencing in normal human keratinocytes triggers metabolic alterations that drive the formation of squamous cell carcinomas. *J Clin Invest* 2011; **121**:195–211.
9 Breitenbach JS, Rinnerthaler M, Trost A *et al.* Transcriptome and ultrastructural changes in dystrophic epidermolysis bullosa resemble skin aging. *Aging (Albany NY)* 2015; **7**:389–411.
10 Maier K, He Y, Wölfle U *et al.* UV-B-induced cutaneous inflammation and prospects for antioxidant treatment in Kindler syndrome. *Hum Mol Genet* 2016; **25**:5339–52.
11 Ng Y-Z, Pourreyron C, Salas-Alanis JC *et al.* Fibroblast-derived dermal matrix drives development of aggressive cutaneous squamous cell carcinoma in patients with recessive dystrophic epidermolysis bullosa. *Cancer Res* 2012; **72**:3522–34.
12 Bernerd F, Asselineau D, Vioux C *et al.* Clues to epidermal cancer proneness revealed by reconstruction of DNA repair-deficient xeroderma pigmentosum skin *in vitro*. *Proc Natl Acad Sci U S A* 2001; **98**:7817–22.
13 Fréchet M, Warrick E, Vioux C *et al.* Overexpression of matrix metalloproteinase 1 in dermal fibroblasts from DNA repair-deficient/cancer-prone xeroderma pigmentosum group C patients. *Oncogene* 2008; **27**:5223–32.
14 Heinemann A, He Y, Zimina E *et al.* Induction of phenotype modifying cytokines by *FERMT1* mutations. *Hum Mutat* 2011; **32**:397–406.
15 Zamarrón A, García M, Del Río M *et al.* Effects of photodynamic therapy on dermal fibroblasts from xeroderma pigmentosum and Gorlin-Goltz syndrome patients. *Oncotarget* 2017; **8**:77385–99.
16 Meana A, Iglesias J, Del Rio M *et al.* Large surface of cultured human epithelium obtained on a dermal matrix based on live fibroblast-containing fibrin gels. *Burns* 1998; **24**:621–30.
17 Robinson MD, Oshlack A. A scaling normalization method for differential expression analysis of RNA-seq data. *Genome Biol* 2010; **11**:R25.
18 Johnson WE, Li C, Rabinovic A. Adjusting batch effects in microarray expression data using empirical Bayes methods. *Biostatistics* 2007; **8**:118–27.
19 Robinson MD, McCarthy DJ, Smyth GK. edgeR: a Bioconductor package for differential expression analysis of digital gene expression data. *Bioinformatics* 2010; **26**:139–40.
20 Benjamini Y, Hochberg Y. Controlling the false discovery rate: a practical and powerful approach to multiple testing. *J Royal Stat Soc B* 1995; **57**:289–300.
21 Alonso R, Salavert F, Garcia-Garcia F *et al.* Babelomics 5.0: functional interpretation for new generations of genomic data. *Nucleic Acids Res* 2015; **43**:W117–21.
22 Huang DW, Sherman BT, Lempicki RA. Bioinformatics enrichment tools: paths toward the comprehensive functional analysis of large gene lists. *Nucleic Acids Res* 2009; **37**:1–13.
23 Hidalgo MR, Cubuk C, Amadoz A *et al.* High throughput estimation of functional cell activities reveals disease mechanisms and predicts relevant clinical outcomes. *Oncotarget* 2017; **8**:5160–78.
24 Szklarczyk D, Franceschini A, Wyder S *et al.* STRING v10: protein–protein interaction networks, integrated over the tree of life. *Nucleic Acids Res* 2015; **43**:D447–52.

25 Escámez MJ, García M, Cuadrado-Corrales N *et al.* The first *COL7A1* mutation survey in a large Spanish dystrophic epidermolysis bullosa cohort: c.6527insC disclosed as an unusually recurrent mutation. *Br J Dermatol* 2010; **163**:155–61.
26 Ashburner M, Ball CA, Blake JA *et al.* Gene ontology: tool for the unification of biology. *Nat Genet* 2000; **25**:25–9.
27 Kanehisa M, Goto S, Sato Y *et al.* KEGG for integration and interpretation of large-scale molecular data sets. *Nucleic Acids Res* 2012; **40**:D109–14.
28 Nyström A, Thriene K, Mittapalli V *et al.* Losartan ameliorates dystrophic epidermolysis bullosa and uncovers new disease mechanisms. *EMBO Mol Med* 2015; **7**:1211–28.
29 Kwon M-J, Kim B, Lee YS, Kim T-Y. Role of superoxide dismutase 3 in skin inflammation. *J Dermatol Sci* 2012; **67**:81–7.
30 Naba A, Clauser KR, Ding H *et al.* The extracellular matrix: tools and insights for the 'omics' era. *Matrix Biol* 2016; **49**:10–24.
31 Lassen N, Bateman JB, Estey T *et al.* Multiple and additive functions of ALDH3A1 and ALDH1A1. *J Biol Chem* 2007; **282**:25668–76.
32 Hoshino Y, Nishida J, Katsuno Y *et al.* Smad4 decreases the population of pancreatic cancer-initiating cells through transcriptional repression of ALDH1A1. *Am J Pathol* 2015; **185**:1457–70.
33 Küttner V, Mack C, Rigbolt KTG *et al.* Global remodelling of cellular microenvironment due to loss of collagen VII. *Mol Syst Biol* 2013; **9**:1–14.
34 Yamaguchi Y. Periostin in skin tissue skin-related diseases. *Allergol Int* 2014; **63**:161–70.
35 González-González L, Alonso J. Periostin: a matricellular protein with multiple functions in cancer development and progression. *Front Oncol* 2018; **8**:225.
36 Tomasek JJ, Gabbiani G, Hinz B *et al.* Myofibroblasts and mechano-regulation of connective tissue remodelling. *Nat Rev Mol Cell Biol* 2002; **3**:349–63.
37 Parsonage G, Filer AD, Haworth O *et al.* A stromal address code defined by fibroblasts. *Trends Immunol* 2005; **26**:150–6.
38 Vong S, Kalluri R. The role of stromal myofibroblast and extracellular matrix in tumor angiogenesis. *Genes Cancer* 2011; **2**:1139–45.
39 Micallef L, Vedrenne N, Billet F *et al.* The myofibroblast, multiple origins for major roles in normal and pathological tissue repair. *Fibrogenesis Tissue Repair* 2012; **5** (Suppl. 1):S5.
40 Kalluri R. The biology and function of fibroblasts in cancer. *Nat Rev Cancer* 2016; **16**:582–98.
41 Mittapalli VR, Madl J, Löffek S *et al.* Injury-driven stiffening of the dermis expedites skin carcinoma progression. *Cancer Res* 2016; **76**:940–51.
42 Küttner V, Mack C, Gretzmeier C *et al.* Loss of collagen VII is associated with reduced transglutaminase 2 abundance and activity. *J Invest Dermatol* 2014; **134**:2381–9.
43 Föll MC, Fahrner M, Gretzmeier C *et al.* Identification of tissue damage, extracellular matrix remodeling and bacterial challenge as common mechanisms associated with high-risk cutaneous squamous cell carcinomas. *Matrix Biol* 2018; **66**:1–21.
44 Midwood KS, Chiquet M, Tucker RP, Orend G. Tenascin-C at a glance. *J Cell Sci* 2016; **129**:4321–7.
45 Yang L, Serada S, Fujimoto M *et al.* Periostin facilitates skin sclerosis via PI3K/Akt dependent mechanism in a mouse model of scleroderma. *PLOS ONE* 2012; **7**:e41994.
46 Naik PK, Bozyk PD, Bentley JK *et al.* Periostin promotes fibrosis and predicts progression in patients with idiopathic pulmonary fibrosis. *Am J Physiol Lung Cell Mol Physiol* 2012; **303**:L1046–56.
47 Ben Q-W, Zhao Z, Ge S-F *et al.* Circulating levels of periostin may help identify patients with more aggressive colorectal cancer. *Int J Oncol* 2009; **34**:821–8.
48 Dong D, Zhang L, Jia L *et al.* Identification of serum periostin as a potential diagnostic and prognostic marker for colorectal cancer. *Clin Lab* 2018; **64**:973–81.
49 Yamaguchi Y, Ono J, Masuoka M *et al.* Serum periostin levels are correlated with progressive skin sclerosis in patients with systemic sclerosis. *Br J Dermatol* 2013; **168**:717–25.
50 Cianfarani F, Zambruno G, Castiglia D, Odorisio T. Pathomechanisms of altered wound healing in recessive dystrophic epidermolysis bullosa. *Am J Pathol* 2017; **187**:1445–53.
51 Bruckner-Tuderman L, Has C. Disorders of the cutaneous basement membrane zone – the paradigm of epidermolysis bullosa. *Matrix Biol* 2014; **33**:29–34.
52 Zapatero-Solana E, García-Giménez JL, Guerrero-Aspizua S *et al.* Oxidative stress and mitochondrial dysfunction in Kindler syndrome. *Orphanet J Rare Dis* 2014; **9**:211.
53 Emmert H, Patel H, Brunton VG. Kindlin-1 protects cells from oxidative damage through activation of ERK signalling. *Free Radic Biol Med* 2017; **108**:896–903.
54 Hosseini M, Ezzedine K, Taieb A, Rezvani HR. Oxidative and energy metabolism as potential clues for clinical heterogeneity in nucleotide excision repair disorders. *J Invest Dermatol* 2015; **135**:341–51.
55 Liu RM, Desai LP. Reciprocal regulation of TGF-β and reactive oxygen species: a perverse cycle for fibrosis. *Redox Biol* 2015; **6**:565–77.
56 Richter K, Kietzmann T. Reactive oxygen species and fibrosis: further evidence of a significant liaison. *Cell Tissue Res* 2016; **365**:591–605.
57 Bergmeier V, Etich J, Pitzler L *et al.* Identification of a myofibroblast-specific expression signature in skin wounds. *Matrix Biol* 2018; **65**:59–74.

Supporting Information

Additional Supporting Information may be found in the online version of this article at the publisher's website:

Fig S1. Pathway activity analysis.

Fig S2. Venn diagram of dysregulated genes in myofibroblasts and genodermatoses fibroblasts.

Table S1. Patient information: age, sex and gene and protein mutations of all patient and control samples.

Table S2. Normalized RNA-Seq counts for all genes and all samples.

Table S3. Differentially expressed genes.

Table S4. Gene ontology and Kyoto Encyclopedia of Genes and Genomes enrichment analysis.

Table S5. Pathway activity analysis.

Powerpoint S1. Journal Club Slide Set.